Hydrolytic Degradation of Pluronic F127/Poly(lactic acid) Block Copolymer Nanoparticles

X. Y. Xiong and K. C. Tam*

School of Mechanical & Production Engineering, Nanyang Technological University, Singapore 639798

L. H. Gan

Natural Sciences, National Institute of Education, Singapore 637616

Received February 18, 2004

ABSTRACT: Poly(lactic acid)s (PLA) were grafted to both ends of Pluronic F127 (PEO−PPO−PEO) to produce novel amphiphilic PLA−F127−PLA block copolymers. The hydrolytic degradation of PLA−F-127−PLA block copolymers in phosphate buffered saline (PBS) (pH 7.4) solution at 37 °C was studied using a combination of physical techniques, such as dynamic light scattering (DLS), transmission electron microscopy (TEM), nuclear magnetic resonance (NMR), and gel permeation chromatography (GPC). It was found that the morphologies and particle size of PLAF127-23 nanoparticles changed dramatically because of the initial rapid degradation of PLA blocks. The morphology of the microstructure transformed from the regular onionlike vesicles to large compound vesicles. With increasing time, the degradation rate of LA−LA linkage was reduced, and the degradation mainly occurred at the interface of F127 and PLA blocks. The morphologies of PLAF127-23 nanoparticles changed from the regular larger compound vesicles to irregular compound vesicles, and to regular large compound vesicles as degradation progresses. Accordingly the particle size of PLAF127-23 nanoparticles decreased initially and remained constant for a certain time period, and it then increased again.

Introduction

Amphiphilic block copolymers have been widely studied in the past several decades due to their excellent capacity to self-assemble to produce nanoparticles containing a hydrophobic core and a hydrophilic shell. Polymeric nanoparticles with good biocompatibility have the potential for many different applications, such as in enhanced drug delivery systems.[1−10] Polyesters such as poly(L-lactic acid) (PLA), polycaprolactone (PCL) and poly(glycolic acid) (PGA) have very good biodegradability and biocompatibility. They can be degraded into small molecules through hydrolytic or enzyme degradation, which are then excreted from the human body by renal clearance. Therefore, amphiphilic block copolymers containing hydrophobic polyester segments have attracted increasing attention from the research community.[11−16] The most widely used hydrophilic polymeric backbone for the grafting of degradable polyesters is poly(ethylene oxide) (PEO) because of its water-solubility and excellent biocompatibility. It is well-known that polyesters degrade rather slowly because of their hydrophobic character. However, it was reported that the degradation rate of polyesters increased when they were grafted to flexible hydrophilic PEO backbones.[15,16] Thus, amphiphilic block copolymers comprising of PEO and polyester segments could be used in various controlled release systems by manipulating the block composition of PEO and polyester.

The degradation properties of film produced from PLA/PEO, PLGA/PEO, and PCL/PEO diblock or triblock copolymers have been studied by only a few research groups.[17−19] The techniques that were commonly used to monitor the degradation process are NMR, GPC, FT-IR, and scanning electron microscope (SEM). Vert et al. studied the hydrolytic and enzymatic degradation of physically cross-linked hydrogels prepared from PLA/PEO/PLA block copolymers using NMR, GPC and FTIR techniques.[20] All the previous studies focused on the degradation behaviors of polymers in the solid or hydrogel form. For drug delivery applications of PEO/polyester block copolymers, it is more useful to examine the degradation properties of nanoparticles in aqueous solution. Up to now, only Wu and co-workers reported the study on the degradation behavior of PCL−PEO−PCL nanoparticles in PBS solution using only the DLS technique.[21,22]

In this paper, amphiphilic block copolymers PLA−PEO−PPO−PEO−PLA were synthesized. The reasons for selecting the PEO−PPO−PEO block instead of hydrophilic PEO are as follows:

1. Poly(ethylene oxide)−poly(propylene oxide)−poly-(ethylene oxide) block copolymer (PEO−PPO−PEO) is a widely used commercial amphiphilic polymer (Pluronics, BASF) that exhibits thermal responsive characteristics.

2. The block copolymer is one of the very few synthetic polymeric materials that is approved by the U.S. Food and Drug Administration for use as food additives and pharmaceutical ingredients.[23]

3. It was reported that poly(ethylene imine)−Pluronic (PEI−Pluronic) block copolymer exhibited higher transfection efficiency toward plasmid DNA than PEI−PEO copolymer due to the amphiphilic property of Pluornic block copolymer.[24] The micelles produced from Pluronic block copolymers have been found to increase the oral and brain bioavailability of drugs.[1] Therefore, PLA−Pluronic−PLA block copolymers are believed to be the better candidates in drug delivery and controlled release systems.

* Corresponding author. E-mail address: mkctam@ntu.edu.sg.

10.1021/ma049662p CCC: $27.50
Published on Web 04/03/2004

Table 1. Characteristics of PLA−F127−PLA Block Copolymers

sample	W_{LA} (% in feed)	W_{LA} (%[a] in product)	unit ratio for PLA:PEO:PPO	$\bar{M}_n$(theory)	$\bar{M}_n$(NMR)	$\bar{M}_w/\bar{M}_n$(GPC)	$\bar{M}_w$[b]	yield (%)
PLAF127-23	50	44.7	142:200:65	25 200	22 800	1.34	30 600	85
PLAF127-29	66.7	57.2	230:200:65	37 800	29 000	1.54	44 700	80
PLAF127-48	80	73.8	500:200:65	50 400	48 000	1.41	67 700	82.5

[a] Determined by the integration ratio of the methyl peak at 1.58 ppm (−O−CH(CH_3)−CO− group in PLA block) and the methyl peak at 1.15 ppm (−OCH_2−CH(CH_3)− group in Pluronic F127 block) in the ^{1}H NMR spectra. [b] $\bar{M}_w = \bar{M}_n$(NMR) × [$\bar{M}_w/\bar{M}_n$(GPC)].

The degradation process of PLA−PEO−PPO−PEO−PLA nanoparticles in PBS solution was examined in details by various physical techniques, such as TEM, DLS, NMR, and GPC. We wish to emphasize that TEM has never been used to study the degradation behavior of these biodegradable polymers. Thus, we report for the first time the microstructural evolution of the morphologies of the aggregate as the degradation progresses.

Experimental Section

Materials. Pluronic F127 was kindly supplied by BASF Corp. (Mount Olive, NJ) and dried overnight under vacuum before use. L-Lactide was purchased from Aldrich and recrystallized from ethyl acetate (EtAc). The purified L-lactide was stored at 4−5 °C under argon environment. Stannous octoate ($Sn(Oct)_2$) was purchased from Aldrich and used as received. Osmium tetroxide (OsO_4) in 2-methyl-2-propanol (2.5 wt %) needed for staining purpose was purchased from Aldrich and used as received.

Synthesis of PLA—F127—PLA Block Copolymers. PLA segments were attached to both ends of Pluronic F127 copolymer to obtain amphiphilic PLA−F127−PLA block copolymers. The detailed synthesis procedure of PLA−F127−PLA block copolymers has been reported previously.[25] A round-bottom flask with a stopcock was heated under reduced pressure to remove the moisture. After cooling to room temperature, argon was introduced into the flask. Following this, appropriate amounts of L-lactide and Pluronic F127 were added and the mixture was heated with continuous stirring to produce a well-mixed molten phase. The mixture was then cooled, and $Sn(Oct)_2$ (0.1 wt % of L-lactide) was added to the flask under argon environment. The mixture was degassed by several vacuum-purge cycles, and then heated to 180 °C. After being stirred for 15 h, the content was cooled to room temperature. The product was dissolved in methylene chloride and precipitated twice in methanol and once in diethyl ether. The polymers were filtered and dried overnight under vacuum.

Hydrolytic Degradation. The nanoparticles of PLA−F127−PLA block copolymers in phosphate buffered saline (PBS, pH 7.4, 0.01 M) aqueous solutions were prepared as follows: PLA−F127−PLA block copolymers were initially dissolved in tetrahydrofuran (THF). The PLA−F127−PLA solutions were added dropwise to PBS solutions under gentle stirring, after which THF was removed under reduced pressure. Then the PLA−F127−PLA copolymers in PBS solutions were mixed continuously in the shaking water bath at 37 °C. At predetermined time intervals, polymer solutions (30 mL) were removed and filtered to remove the insoluble degraded PLA blocks. The filtrate solutions were dried and dissolved in $CDCl_3$ for NMR measurement and THF for GPC measurement, respectively. The insoluble inorganic salts from PBS solutions were filtered before NMR and GPC measurements. The PBS was used as it simulates the condition of the human body and it mediates any fluctuations from the H^+ and OH^- ions released during the degradation process.

Characterization. Nuclear magnetic resonance (NMR) spectra were recorded at room temperature using a Bruker ACF-400 (400 MHz) Fourier transform spectrometer. Chemical shifts (δ) were given in ppm using tetramethylsilane (TMS) as the internal reference. GPC of the copolymers was performed on an Agilent 1100 apparatus equipped with a differential refractometer as the detector. Tetrahydrofuran (THF) was used as the mobile phase with a flow rate of 1.0 mL/min.

Dynamic Light Scattering. The frequency of scattered light fluctuates around the incident light due to the constant motion of the polymer molecules. Dynamic light scattering (DLS) measures the intensity fluctuations with time and correlates these fluctuations to the properties of the scattering objects. In general, the terms of correlation functions of dynamic variables are always used to describe the response of the scattering molecules to the incident light. From the expression

$$\Gamma = Dq^2 \tag{1}$$

the translational diffusion coefficients, D can be determined. Γ is the decay rate, which is the inverse of the relaxation time, τ, q the scattering vector ($q = (4\pi n \sin(\theta/2))/\lambda$), where θ is the scattering angle, n is the refractive index of the solution, and λ is the wavelength of the incident light. If the Stokes−Einstein equation is used, the apparent hydrodynamic radius, R_h, can be calculated using the following equation:

$$R_h = \frac{kT}{6\pi\eta D} \tag{2}$$

where k is the Boltzmann constant, T the absolute temperature, and η the solvent viscosity.

A Brookhaven BIS200 laser scattering system was used to perform the static and dynamic light scattering experiments. The light source is a power adjustable vertically polarized 350 mW argon ion laser with a wavelength of 488 nm. The inverse Laplace transform of REPES supplied with the GENDIST software package was used to analyze the time correlation function (TCF), and the probability of reject was set to 0.5.

Transmission Electron Microscope (TEM). TEM was performed on a JEOL JEM-2010 electron microscope at an acceleration voltage of 200 kV. The copper grid (400 meshes) with a carbon film was used. The copper grid was immersed in a drop of the aqueous polymer solution for 2 min, and then removed and dried. A drop of osmium tetroxide (OsO_4) in 2-methyl-2-propanol (2.5 wt %) was placed on the copper grid for 2 min. The copper grid was then dried overnight at room temperature prior to measurement.

Results and Discussion

The block copolymers PLA−F127−PLA were synthesized by ring-opening polymerization of the monomer L-lactide using Pluronic copolymer F127 as the initiator and stannous octoate ($Sn(Oct)_2$) as the catalyst. The polymer composition, structure and molecular weight were characterized by NMR and GPC techniques and summarized in Table 1.

The hydrolytic degradation of nanoparticles formed from PLA−F127−PLA block copolymers in PBS solutions (pH 7.4) at 37 °C were examined in details by DLS, TEM, NMR and GPC over a time period of about two months.

The change in the hydrodynamic radius (R_h) of PLA−F127−PLA nanoparticles with degradation was examined by DLS. The concentration used in the laser light

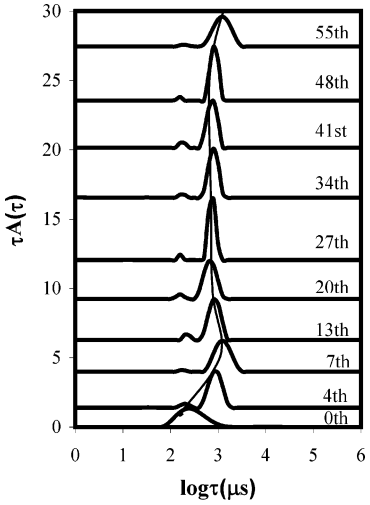

Figure 1. Relaxation time distribution functions of PLAF127-23 block copolymer in aqueous solution (0.1 wt %) at 90° measured at different degradation times.

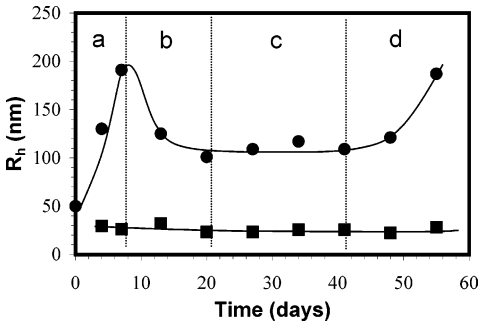

Figure 2. Changes in the hydrodynamic radius (R_h) of PLAF127-23 aggregates as a function of degradation times.

scattering experiments is 0.1 wt %, which is in the dilute solution regime.

Figure 1 shows the relaxation time distribution functions of PLAF127-23 block copolymer in PBS solution measured at a scattering angle of 90°. Only one single peak was evident before the degradation commences. We had previously confirmed from TEM micrographs that this single peak corresponds to onionlike vesicles containing three layers.[25] However, on the fourth day, the size and distribution of particles exhibited an obvious change, where two peaks were detected and they remained unchanged over the remainder two months. The peak corresponding to the large aggregate became narrower between the fourth to 27th day, and it then became broader until the 55th day. The change in the size (R_h) of nanoparticles as degradation progressed is shown in Figure 2. The particle size (R_h) of large aggregate increased dramatically from 50 to 191 nm during the first 7 days. It progressively decreased to a minimum on the 20th day where the particle size remained essentially constant (R_h ~100 nm) for about 20 days. After the 41st day, the particle size (R_h) increased again to a size of ~ 187 nm on the 55th day. However, no significant change in the size of small particles was observed over the 2 month period.

To understand the changes in the morphologies of PLA−F127−PLA nanoparticles with degradation time, samples were removed and examined by TEM. The hydrophobic PLA segments containing double bonds were stained with OsO_4 and the TEM micrographs of PLAF127-23 aggregates as a function of degradation time are shown in Figure 3. Before the hydrolytic degradation, PLAF127-23 nanoparticles exist as onion-like vesicle with three layers.[25] On the seventh day of degradation, two kinds of particle size distribution were observed in the TEM micrographs. The morphology of nanoparticles became regular large compound vesicles with diameter of around 350 and 60 nm, respectively. The morphology of PLAF127-23 aggregates remained unchanged up to the 20th day, but the size of large particles decreased to ~200 nm. With further degradation from the 27th to 41st day, the morphologies of nanoparticles became irregular compound vesicles and were rather complicated, where the diameter is about 200 and 60 nm, respectively. PLAF127-23 aggregates reassembled into regular large compound vesicles on the 55th day, where the diameter of large particles increased to ~350 nm. The morphologies and size of particles determined from TEM is corroborated by the results measured using the DLS technique.

Table 2. NMR Results of PLAF127-23 Copolymer at Various Hydrolytic Degradation Times

degradation time (days)	normalized integration ratio of peaks d:c:a	av. EO-LA linkages per molecule (N)[a] (%)	approx $\bar{M}_n$(PLA) on both ends[b]
0	995:4:142	100	10200
7	995:4:66	100	4800
20	995:3.8:55	95	4200
55	995:2.5:38	62	4400

[a] N = (integration value of peak c) × 100/4 [b] $\bar{M}_n$(PLA) = 72 × (integration value of peak a)/N.

The degradation samples were also examined by NMR and GPC in order to determine the mechanism of degradation by examining the chemical composition and size distribution of the polymer chains. Figure 4 shows the NMR spectra of the degradation mixture of PLAF127-23 block copolymer from the seventh to 55th day of degradation. There are two possible degradation sites on the PLA−F127−PLA block copolymer; namely at the middle of PLA block (LA−LA linkage) and at the interface of PLA and F127 blocks (LA-EO linkage) as indicated below:

EO-LA bond:

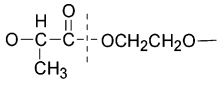

LA-LA bond:

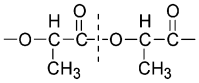

We believe that the LA−LA bond cleavage occurred first since the EO−LA bond is more stable than LA−LA bond. As shown above, it could be that the EO group (−CH_2CH_2O−) next to the ester group makes the EO−LA bond more stable than the LA group (−$CH(CH_3)$−$C(O)$−) in the LA−LA bond. Therefore, in the degraded samples, the possible compounds that may be present after degradation are PLA−F127−PLA, PLA−F127, F127, and fragmented LA segments (one to two repeating units of LA). The insoluble fragments of degraded LA segments have been removed by filtration. The results obtained from NMR are summarized in Table 2. The small peak "c" at δ of 4.2−4.3 ppm belongs to the methylene protons of PLA-CO−OCH_2−CH_2−O−F127- segment. Peaks "a" and "d" belong to the methine proton of PLA blocks (O−CH(CH_3)−CO−: δ = 5.15−5.19 ppm) and the methyl protons of F127 block (−OCH_2− CH_2− and −OCH_2−CH(CH_3)−: δ = 3.35−3.75 ppm). From the integration ratio of peaks "c" and

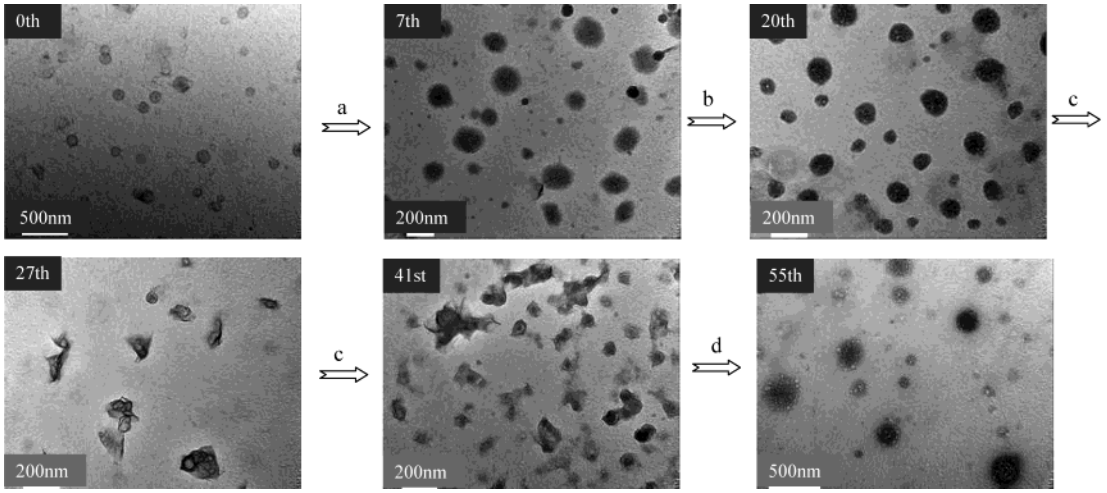

Figure 3. TEM micrographs of PLAF127-23 aggregates at different degradation times. The numbers shown at the upper corner of TEM pictures represents the degradation time.

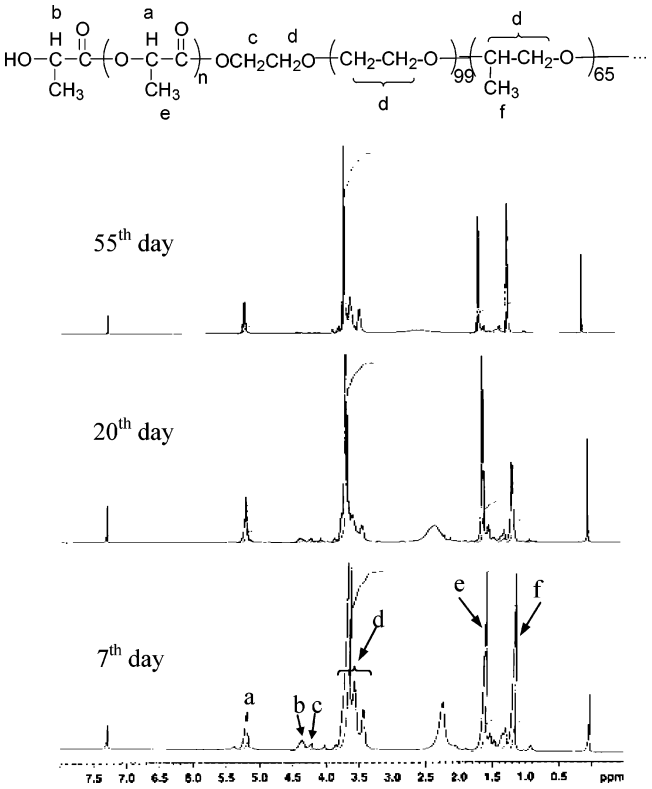

Figure 4. ^{1}H NMR spectra of PLAF127-23 block copolymer with degradation ($CDCl_3$).

"d", the approximate molar content of PLA−F127−PLA (N) on the different degradation time was calculated. Before the degradation, the integration ratio of peaks "c" and "d" is 4:995. As degradation progressed, the integration value of peak "c" decreased to 3.8 on the seventh day. Therefore, the approximate molar content of PLA−F127−PLA (N) present in the degradation mixture is 95% (= 3.8/4). The averaged $\bar{M}_n$ of PLA blocks in PLA−F127−PLA block copolymers was derived from the integration ratio of peaks "a", "c", and "d". It should be pointed out that the segment length of PLA blocks on both ends of PLAF127-23 copolymer may be different after hydrolytic degradation, as one would not expect identical scission of the LA segments during the degradation process. Thus, the $\bar{M}_n$ of PLA blocks shown in Table 2 is the mean value of PLA blocks at the ends of the Pluronic polymer chains. From the NMR results in

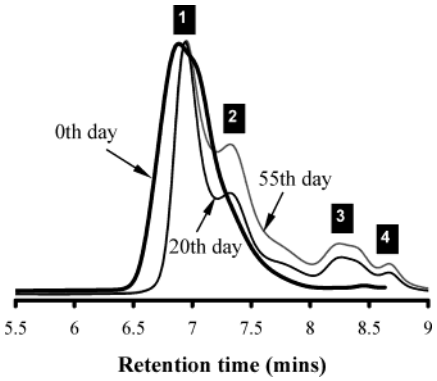

Figure 5. GPC traces (RI signal) of PLAF127-23 block copolymer at 20 and 55 days of hydrolytic degradation.

Table 2, the degradation occurred mainly at the LA−LA linkage on the seventh day of degradation where the $\bar{M}_n$ of PLA blocks decreased rapidly from 10200 to 4800 Da. The initial rapid degradation of PLA blocks was also reported by Li et al.[26] for thin slabs of PLA−PEO−PLA block copolymers. On the 20th day, the degradation occurred mainly at the LA−LA linkage and less than 5% of PLAF127−23 degraded at the EO−LA linkage. Beyond the 20th day, the degradation rate was reduced and the degradation mainly occurred at the EO−LA linkage. About 38% of PLA−F127−PLA block copolymer had degraded on the 55th day due to the cleavage of EO−LA linkage. The $\bar{M}_n$ of PLA blocks in PLA−F127−PLA block copolymer remained unchanged beyond the 20th day.

The degraded samples of PLAF127-23 block copolymer were analyzed using the GPC. Figure 5 shows the GPC traces of PLAF127-23 during the hydrolytic degradation process. On the 20th day, the GPC curve exhibited four different peaks (peaks 1, 2, 3, and 4 as marked) when compared to a single peak observed for the virgin PLAF127-23 solution. The main distribution peak (1) had obviously shifted to the right side, confirming the scission of the PLAF127-23 chains. Three peaks (2−4) corresponding to smaller molecular weight fragments were also observed, and the retention time of these three peaks remained unchanged. However, the intensity of the peak increased with degradation time. The GPC curve did not change much on the 55th day while the intensity of peak 1 decreased slightly and intensity of peaks 2, 3, and 4 increased. This indicated

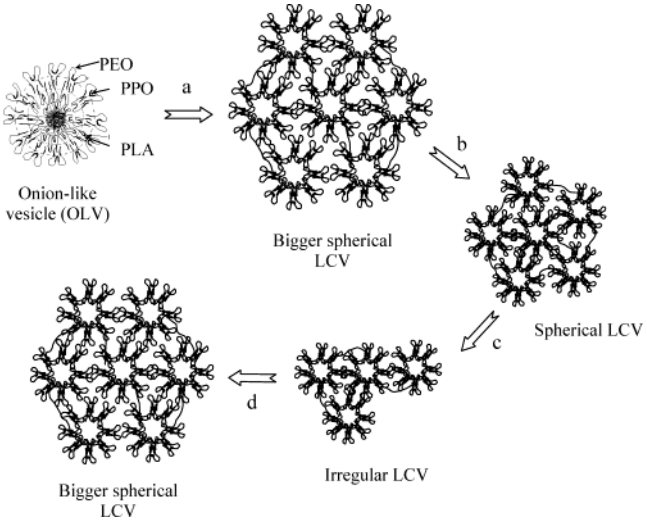

Figure 6. The schematic representation for the aggregation mechanism of the PLAF127-23 block copolymer at different degradation times.

Table 3. Lorentzian Fitting Results of GPC Curves in Figure 5 Determined from the Origin Software

	peak area (%)			
time (days)	[1]	[2]	[3]	[4]
20	47	35	16	2
55	35	46	18	1

that the molecular weight of PLA−F127−PLA copolymer remained unchanged while the weight content of PLA−F127−PLA copolymer decreased. Such trend corroborated with our earlier finding from NMR that the primary degradation occurred at the interface of Pluronic and PLA blocks. Accordingly the content of compounds with smaller molecular weight fragments increased. The GPC curves in Figure 5 were analyzed by Origin software and the four peaks were fitted by Lorentzian formulation, where the curves were deconvoluted into separate curves with identifiable peak. The fractional areas of the four peaks at different degradation times are summarized in Table 3. The area of peak 1 decreased from 47% on the 20th day to 35% on the 55th day while the area of peak 2 increased from 35% to 46%. These results are in agreement with that determined from NMR.

On the basis of the results obtained from DLS, TEM, NMR, and GPC, a probable degradation mechanism of PLAF127-051 block copolymer is given below, and the pictorial representation is shown in Figure 6.

1. In the process step "a" (from the zeroth to the seventh day), the particle size and morphology of PLAF127-23 block copolymer rapidly change due to the high degradation rate of PLA blocks (LA−LA linkage). Because of the dramatic reduction in the length of PLA blocks, hydrophobic interaction of PLA segments is significantly reduced and is not sufficient to produce regular onionlike vesicles. Therefore, additional polymer chains self-assemble to form more complicated large compound vesicles, as correlated by the large increase in the particle size of PLAF127-23 system.

2. With further degradation (process step "b", from the seventh to the 20th day), the cleavage rate of LA−LA linkage decreases significantly and the degradation at the interface of PLA and F127 blocks (EO−LA linkage) dominates. The morphology of nanoparticles remained unchanged due to the slow degradation rate of both LA−LA and EO−LA linkages. However, the particle size exhibited a large decrease from the seventh to the 20th day. We believed that the polymer chains reorganized to form more stable and uniform aggregates containing lower aggregation number because of the cleavage of EO−LA linkages.

3. In step "c" (from the 20th to the 41st day), the cleavage rate of EO−LA linkage increases and large compound vesicles are destroyed to produce irregular shaped compound vesicles.

4. With further degradation (step "d", from the 41st to the 55th day), the hydrophobic interaction of PLA blocks is further weaken, thus more polymer chains aggregated together to form spherical large compound vesicles, resulting in an increase in the particle size.

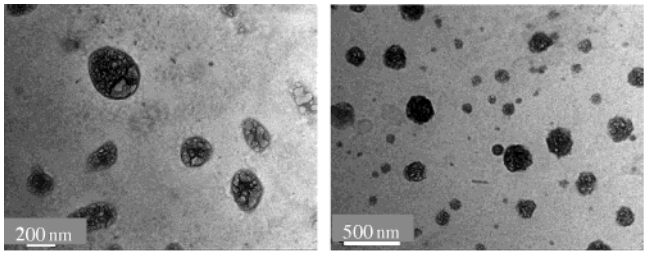

Figure 7. TEM micrographs of PLAF127-29 (A) and PLAF127-48 (B) nanoparticles on the third day of hydrolytic degradation.

The degradation behaviors of PLAF127-29 and PLAF127-48 block copolymers were also examined by TEM (see Figure 7). Large compound vesicles were also observed after the third day for both polymers, which are consistent with the results observed from PLAF127-23 block copolymer. The study on the hydrophobic and hydrophilic drug release behaviors of PLA−F127−PLA block copolymers in vitro is currently in progress.

Conclusions

The hydrolytic degradation behavior of PLAF127-23 block copolymer in PBS (pH 7.4) solution at 37 °C was studied in detail by DLS, TEM, NMR, and GPC. The degradation mechanism of the PLAF127-23 block copolymer is proposed. The initial rapid degradation of the LA−LA linkage resulted in the dramatic change in the morphologies and particle size of PLAF127-23 nanoparticles. The morphologies transformed from regular onionlike vesicles to large compound vesicles, and accordingly, the particle size (R_h) increased from 50 to 191 nm. With further degradation, the cleavage of the EO−LA linkage dominated. The regular larger compound vesicles formed from PLAF127-23 were destroyed and became irregular compound vesicles. With the continuous degradation at the interface of PLA and F127 blocks, the hydrophobic interaction of PLA blocks is weakened. Therefore, irregular vesicles aggregated together to form regular large compound vesicles and the particle size increased correspondingly. The initial change in the morphologies with the degradation for PLAF127-29 and PLAF127-48 block copolymers is in agreement with that observed for the PLAF127-23 block copolymer.

Acknowledgment. We would like to acknowledge the financial support in the form of a SDS grant from the school of MPE. X.Y.X. would like to thank NTU for the financial support in the form of a Ph.D. graduate scholarship.

References and Notes

(1) Rosler, A,; Vandermeulen, G. W. M.; Klok, H. A. *Adv. Drug Deliv. Rev.* **2001**, *53*, 95−108.
(2) Discher, D. E.; Eisenberg, A. *Science* **2002**, *297*, 967−973.
(3) Gan, Z. H.; Jim, T. F.; Li, M.; Yuer, Z.; Wang, S. G.; Wu, C. *Macromolecules* **1999**, *32*, 590−594.
(4) Bae, Y. H.; Huh, K. M.; Kim, Y.; Park, K. H. *J. Controlled Release* **2000**, *64*, 3−13.
(5) Lee, S. H.; Kim, S. H.; Kim, Y. H. *Macromol. Res.* **2002**, *10*, 85−90.
(6) Kabanov, A. V.; Batrakova, E. V.; Alakhov, V. Y. *Adv. Drug Deliv. Rev.* **2002**, *54*, 759−779.
(7) Yekta, A.; Xu, B.; Duhamel, J.; Adiwidjaja, H.; Winnik, M. A. *Macromolecules* **1995**, *28*, 956−966.
(8) Neradovic, D.; van Steenbergen, M. J.; Vansteelant, L.; Meijer, Y. J.; van Nostrum, C. F.; Hennink, W. E. *Macromolecules* **2003**, *36*, 7491−7498.
(9) Lele, B. S.; Leroux, J. C. *Macromolecules* **2003**, *35*, 6714−6723.
(10) Rangelov, S.; Almgren, M.; Tsvetanov, C.; Edwards, K. *Macromolecules* **2003**, *35*, 4770−4778.
(11) Choi, S. K.; Kim, D. *J. Appl. Polym. Sci.* **2002**, *83*, 435−445.
(12) Huang, M. H.; Suming, L. M.; Coudane, J.; Vert, M. *Macromol. Chem. Phys.* **2003**, *204*, 1994−2001.
(13) Wan, Y. Q.; Chen, W. N.; Yang, J.; Bei, J. Z.; Wang, S. G. *Biomaterials* **2003**, *24*, 2195−2203.
(14) Kim, S. Y.; Kim, J. H.; Kim, D.; An, J. H.; Lee, D. S.; Kim, S. C. *J. Appl. Polym. Sci.* **2002**, *82*, 2599−2605.
(15) Li, S. M.; Garreau, H.; Pauvert, B.; McGrath, J.; Toniolo, A.; Vert, M. *Biomacromolecules* **2002**, *3*, 525−530.
(16) Wang, S. G.; Chen, H. L.; Cai, Q.; Bei, J. Z. *Polym. Adv. Technol.* **2001**, *12*, 253−258.
(17) Kissel, T.; Li, Y. X.; Unger, F. *Adv. Drug Deliv. Rev.* **2002**, *54*, 99−134.
(18) Anderson, J. M.; Shive, M. S. *Adv. Drug Deliv. Rev.* **1997**, *28*, 5−24.
(19) Witt C, Kissel, T. *Eur. J. Pharmacol. Biopharm.* **2001**, *51*, 171−181.
(20) Li, S. M.; Molina, I.; Martinez, M. B.; Vert, M. *J. Mater. Sci.—Mater. M.* **2002**, *13*, 81−86.
(21) Nie, T.; Zhao, Y.; Xie, Z. W.; Chi, W. *Macromolecules* **2003**, *36*, 8825−8829.
(22) Zhao, Y.; Hu, T. J.; Lv, Z.; Wang, S. G.; Wu, C. *J. Polym. Sci., Polym. Phys.* **1999**, *23*, 3288−3293.
(23) Alexandridis, P.; Hatton, T. A. *Colloids Surf.* **1995**, *96*, 1−46.
(24) Nguyen, H. K.; Lemieux, P.; Vinogradov, S. V.; Gebhart, C. L.; Guerin, N.; Paradis, G.; Bronich, T. K.; Alakhov, V. Y.; Kabanov, A. V. *Gene Ther.* **2000**, *7*, 126−138.
(25) Xiong, X. Y.; Tam, K. C.; Gan, L. H. *Macromolecules* **2003**, *36*, 9979−9985.
(26) Li, S. M.; Anjard, S.; Rashkov, I.; Vert, M. *Polymer* **1998**, *39*, 5421−5430.

MA049662P